How Very Low-Energy (0.1–2 eV) Electrons Cause DNA Strand Breaks

Jack Simons

Chemistry Department, University of Utah, Salt Lake City, UT 84112, USA
E-mail: simons@chemistry.utah.edu
URL: http://simons.hec.utah.edu

Abstract

Our recent theoretical and others' experimental findings are overviewed concerning the mechanisms by which very low-energy (0.1–2 eV) free electrons attach to DNA and cause strong (ca. 4 eV) covalent bonds to break. The computational tools needed to deal with the metastable shape resonance anions that arise in these processes are discussed and illustrations of their applications to the particular case of DNA damage are provided. Our primary conclusions are that (i) attachment to base π^* orbitals in the above energy range most likely results in cleavage of sugar-phosphate C–O σ bonds, (ii) the rates of C–O bond cleavage can be as high as 10^{10} s^{-1}, and (iii) bond cleavage initiated by electron attachment to phosphate P=O π bonds is less likely involved. The experiments that motivated our theoretical work are discussed as are later experimental findings that confirm our predictions about the nature of the electron attachment event and about which bonds break when strand breaks form.

Contents

1. INTRODUCTION

In the past few years, the author's research group has been involved in [1–5] using electronic structure theory to characterize mechanisms by which electrons with kinetic energies in the 0.1 to 2 eV range attach to and subsequently fragment strong chemical bonds (e.g., having dissociation energies near 4 eV) in DNA. Our work in this area was inspired by very novel experimental findings [6] from the Sanche group in which strand breaks in dried (i.e., having only the structural water molecules intact) DNA were produced by electrons having

ADVANCES IN QUANTUM CHEMISTRY, VOLUME 52
ISSN: 0065-3276 DOI: 10.1016/S0065-3276(06)52008-8

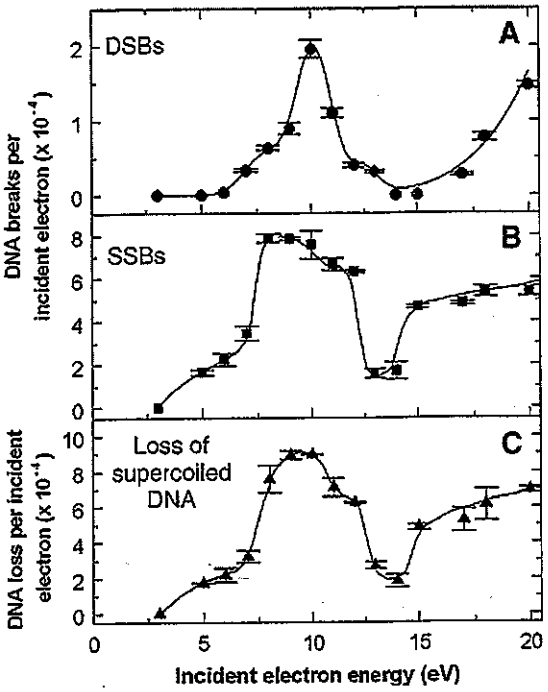

Fig. 1. The yield of single strand breaks (middle panel) per attached electron as a function of the kinetic energy of the incident electron (taken from Fig. 1 of Ref. [6]).

kinetic energies as low as 3.5 eV. The yields of single strand breaks (SSBs) were observed to depend on the energy of the incident electron in a manner (see Fig. 1) that suggested (because peaks and valleys appeared) some kind of resonant process was involved.

Based on the energies at which the peaks in the SSB plots occurred, it was suggested that the bond breaking that causes the SSB is initiated by the incident electrons attaching to the DNA bases' π^* orbitals to form core-excited resonance states (e.g., as in $e^- + \pi^2 \rightarrow \pi^1\pi^{*2}$).

However, we knew from data of the Burrow group [7] that electrons of even lower kinetic energies can attach to low-lying π^* orbitals of the bases of DNA to form shape resonance anions. In particular, the Burrow data indicated that all DNA bases have shape resonance states lying considerably below (e.g., in the 0.1–2 eV range as shown in Fig. 2) the 3.5 eV strand break threshold found in the Sanche experiments. This led us to wonder whether even lower energy electrons than used in Ref. [6] could induce strand breaks in DNA by forming shape rather than core-excited resonances.

2. WHERE DO VERY LOW-ENERGY ELECTRONS ATTACH TO DNA AND WHAT BONDS ARE BROKEN?

Knowing that shape resonances typically have shorter lifetimes (with respect to autodetachment) than core-excited resonances, we anticipated finding that although the DNA bases indeed can attach electrons at energies considerably below 3.5 eV, the shape reso-

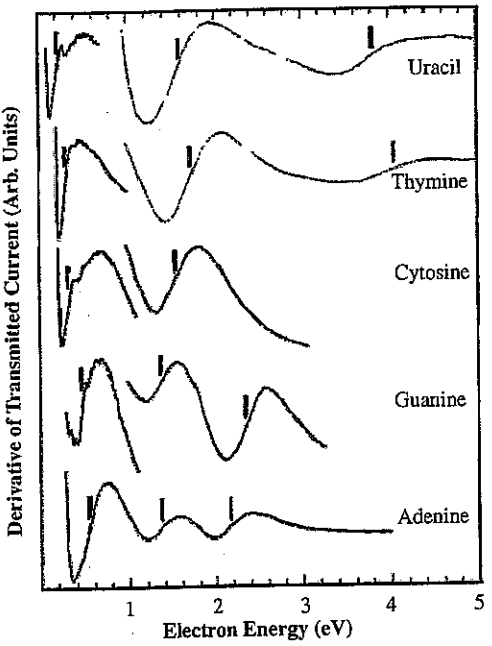

Fig. 2. The electron transmission spectra of the four DNA bases showing the energies (vertical lines) at which the low-energy π^* orbitals occur (taken from Fig. 1 of Ref. [7]).

nances thus formed decay so quickly that the yield of bond breakage is extremely low. This would be consistent with the Sanche data showing no strand break yield in the energy range where shape resonances are expected. Nevertheless, because it was clear to us from Ref. [6] that experimental limitations precluded those workers observing strand breaks at such lower energies, we decided to explore this possibility further, and our results are detailed in Refs. [1–5].

2.1. The DNA fragments studied

In each of our studies, we examined a fragment of DNA using ab initio electronic structure methods to determine which bond(s) would be most susceptible to cleavage when an electron is attached to a low-energy π^* orbital. The fragments included

a. the cytosine (C)–sugar–phosphate fragment shown in Fig. 3a,
b. an analogous fragment with cytosine replaced by thymine (T) (C and T have the lowest-lying π^* orbitals, so we began our studies with them),
c. the fragment containing three π-stacked C bases shown in Fig. 3b, and
d. the sugar–phosphate–sugar fragment shown in Fig. 3c.

We undertook the latter study because we wanted to address the relative probabilities for electron attachment to the phosphate group's P=O π^* or to a base π^* orbital.

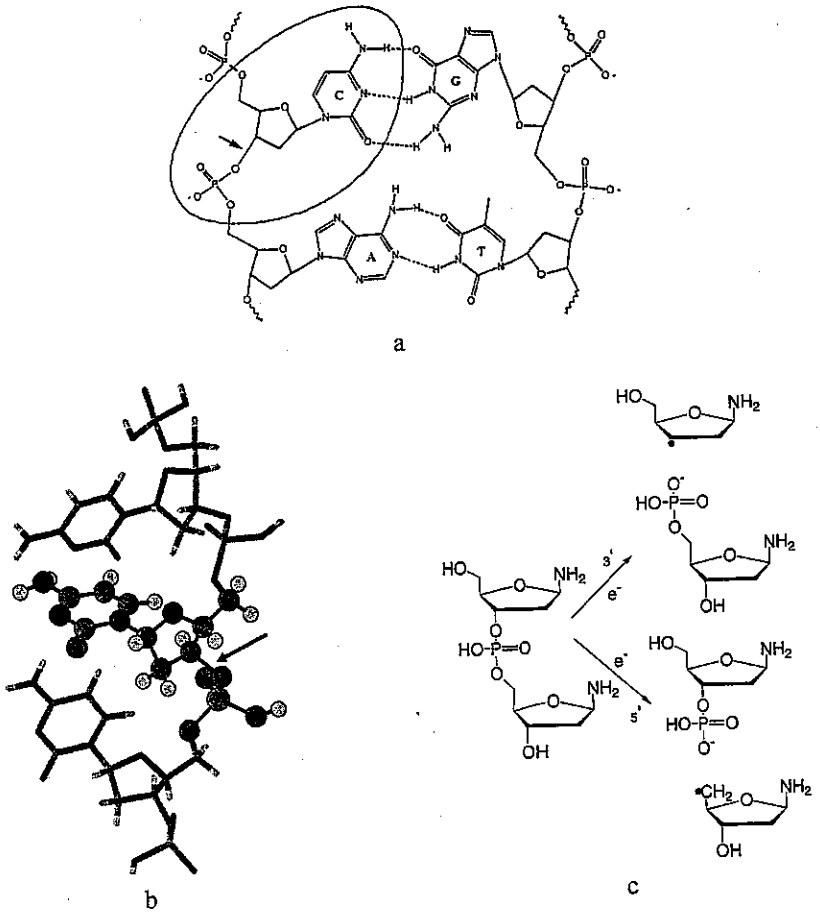

Fig. 3. DNA fragments studied in Refs. [1–5] (see text for explanation). a: taken from Ref. [1], Fig. 1; b: taken from Ref. [4], Fig. 4; c: redrawn figure from Ref. [8].

2.2. Review of our findings

The primary findings of our efforts were that:

a. Attachment of electrons in the 0.1–2 eV range (into C or T π^* orbitals) to form shape resonances can produce covalent bond cleavages.
b. A sugar-phosphate C–O σ bond is the bond whose cleavage requires surmounting the lowest barrier (i.e., in the 0.2–1 eV range, depending on the energy at which the electron attaches to the base within the Heisenberg width of the shape resonance).
c. Cleavage of a base-sugar N–C bond can also occur, but at significantly lower rates because this bond cleavage requires surmounting a larger barrier than for the sugar-phosphate C–O bond.
d. The thermodynamic driving force that causes the sugar–phosphate C–O bond to have the lowest barrier is the huge (ca. 5 eV) electron affinity of the phosphate radical generated by breaking this C–O bond.

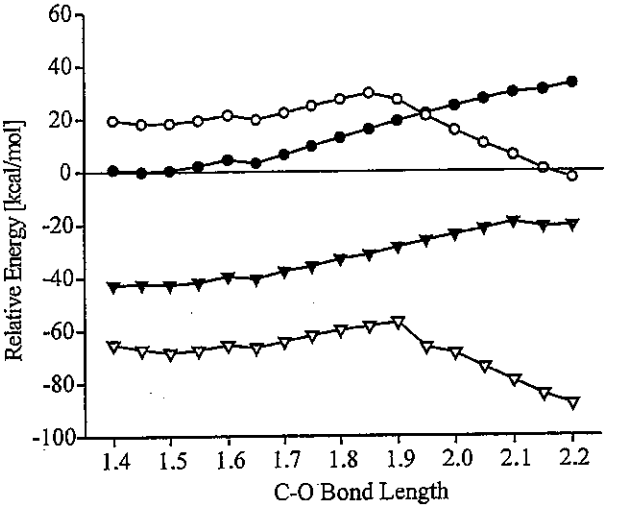

Fig. 4. Energies of neutral (filled symbols) and anionic (open symbols) cytosine-containing DNA fragment of Fig. 3a vs. C–O bond length (Å) in the absence of any solvation (top two plots) and with solvation characterized by dielectric constant $\varepsilon = 78$ (bottom two plots). Taken from Ref. [1], Fig. 2.

e. Electron attachment to the P=O π bond of the phosphate moiety requires electrons of considerably higher energy (> 2 eV) than for attachment to base π^* orbitals.
f. The fraction of C–O σ bond that cleave when an electron is attached, which is determined from the relative rates for surmounting the barrier noted above and the rates of autodetachment, can be as high as 10^{-4} for electrons in the 1 eV range.

2.3. Our proposed mechanism for sugar–phosphate C–O σ bond cleavage

To understand how electrons having kinetic energies in the 0.1–2 eV range can fragment a C–O σ bond whose dissociation energy is ca. 4 eV, we show in Fig. 4 some potential energy profiles that are characteristic of all of the findings of Refs. [1–5].

Let us focus on the top two plots in Fig. 4, which relate to the cytosine–sugar–phosphate fragment shown in Fig. 3a in the absence of any solvation (as appropriate to the experiments of Ref. [6]). The potential energy profiles appropriate to the thymine–sugar–phosphate fragment as well at the two fragments shown in Figs. 3b and 3c display similar characteristic shapes (i.e., the electron-attached state's energy rises, passes over a barrier, and then falls) although the heights of the barriers differ from fragment to fragment. The essential issue to understand is what causes these profiles to have barriers and what determines how steeply the curves fall at large R.

The data represented by the filled circles in Fig. 4 describe the variation in the energy of the neutral cytosine–sugar–phosphate unit in the absence of any attached electron as a function of the sugar–phosphate C–O bond length (R). If followed to much larger R-values, the energy of this curve approaches ca. 90 kcal mol^{-1}, which is the dissociation energy for homolytic cleavage of the C–O bond. The data represented by the open circles

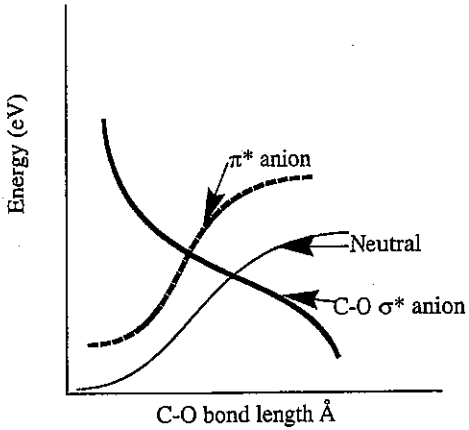

Fig. 5. Qualitative plots of the (diabatic) energies of the anion states in which the excess electron occupies the base π^* orbital and in which the electron occupies the C–O σ^* orbital as well as the variation of the energy of the neutral molecule.

in Fig. 4 describes the variation in the energy of the corresponding unit with an electron attached. Specifically, the electron has been placed into a π^* orbital of the cytosine base lying (vertically) ca. 1 eV above the energy of the neutral thus forming a metastable shape resonance.[1]

If the attached electron is forced (e.g., by constraining the orbital occupancy used in our wave function to retain its π^{*1} character) to remain in the cytosine π^* orbital, the energy of this electron-attached state would parallel that of the neutral molecule and rise by nearly 90 kcal mol^{-1} as the C–O bond cleaves. However, because our quantum wave function allows the orbital occupancy of all the electrons to be optimized, something different happens. As suggested qualitatively in Fig. 5, another anion state in which the excess electron occupies the C–O σ^* orbital also comes into play as the C–O bond is stretched.

Specifically, near the equilibrium C–O bond length, the σ^*-attached anion is much higher in energy than is the π^*-attached anion; this is why the shape resonance state at 1 eV is a base π^* state. However, as the C–O bond lengthens, its σ orbital rises in energy and its σ^* orbital decreases in energy; the latter being shown in Fig. 5. The rate at which the σ^* orbital falls as R increases is determined by the electron affinity of the phosphate radical that forms when the C–O bond breaks. At a C–O bond length near 1.9 Å (see Fig. 4), the π^{*1} and σ^{*1} anion states' diabatic energies become equal. It is near such a crossing that the configuration interaction (CI) between these two states is strongest. The resulting CI, which is automatically included in our ab initio calculation, allows the wave function to smoothly evolve from π^{*1} to σ^{*1} character as R passes through the crossing region. Again, it is important to emphasize that the reason the σ^*-attached anion's energy drops strongly as R increases lies in the very high (ca. 5 eV) electron affinity (EA) of the oxygen site of the phosphate radical. In fact, it is because the phosphate radical's EA is considerably larger than the EA of the base nitrogen-centered radical formed when a base-sugar N–C

[1] By eliminating the outgoing continuum component of the basis functions used to describe this state, we are able to force the attached electron to remain in the π^* orbital as we subsequently stretch the C–O bond to generate the open-circles data.

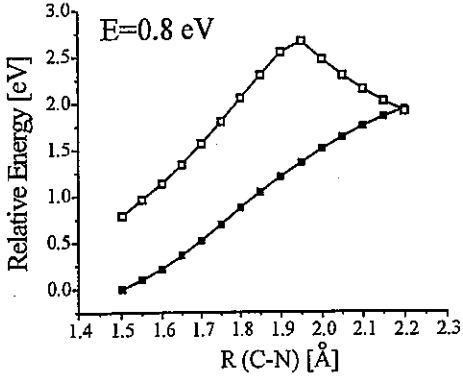

Fig. 6. Energy profile for the neutral (filled squares) and anion (open squares) thymine–sugar–phosphate unit as a function of the thymine–sugar C–N bond length (taken from Fig. 7 of Ref. [4]).

bond breaks that the barrier to sugar–phosphate C–O bond cleavage is lower than that for base-sugar N–C bond cleavage. An example of the energy profile for C–N bond cleavage in the thymine–sugar–phosphate system studied in Ref. [4] is shown in Fig. 6 for the case in which 0.8 eV electrons attach to the thymine π^* orbital.

In summary, the strand breaks we studied are generated when

a. an electron having kinetic energy appropriate to enter a low-lying π^* orbital of a DNA base strikes and enters such an orbital to form a shape resonance, after which
b. a through-bond electron transfer event occurs if the sugar–phosphate C–O σ bond is elongated (e.g., through normal vibrational motions) to near 1.9 Å allowing a barrier to be surmounted and π^*/σ^* configuration interaction to take place,
c. producing a σ^*-attached anion that promptly fragments to yield a carbon radical and a (very stable) phosphate-site anion.

The rate of the through-bond electron transfer from the base π^* to the sugar–phosphate C–O σ^* orbital was estimated by examining the avoided crossing of the π^* and σ^* anion states near the C–O bond length of 1.9 Å. The energy splitting δE was then used to compute the rate and values in the 10^{13} s^{-1} were obtained. As we show later, this through-bond transfer rate is considerably faster than the rate at which the barrier on the anion's energy surface near 1.9 Å is surmounted, so the latter is the rate-limiting event in producing SSBs.

2.4. Subsequent experimental verifications

To our pleasure, subsequent to our studies suggesting that shape resonances could induce strand breaks in DNA, new measurements [9] were carried out at even lower electron kinetic energies and strand breaks were indeed observed as Fig. 7 illustrates.

Because the DNA samples used in Refs. [6] and [9] contained all four bases, it was not possible to infer whether the electron attachment takes place at any particular base(s). However, because all four bases have their lower-energy π^* resonance states in the 0.1–2 eV range, the data strongly suggest that the strand breaks are taking place by formation of such π^* shape resonances as our earlier predictions claimed. In fact, in Ref. [9] it is

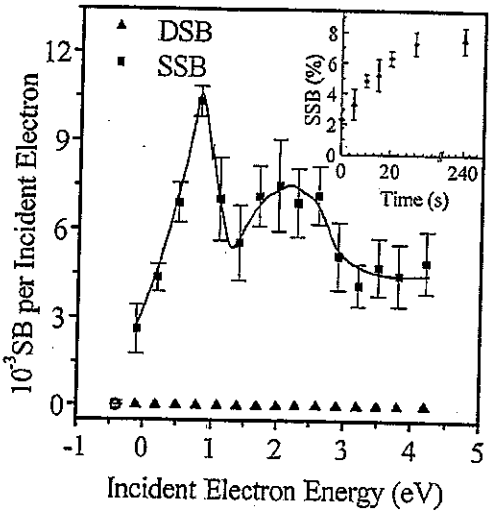

Fig. 7. Yield of DNA strand breaks as a function of electron kinetic energy showing SSBs occurring in the 0.1–2 eV range studied in Refs. [1–5] (taken from Fig. 1 of Ref. [9]).

even emphasized that the shape of the strand-break yield plot of Fig. 7 is quite similar to the known shape of the DNA bases' electron attachment cross-sections, further supporting our claim that it is to the base π^* (and not[2] phosphate P=O π^* or any σ^*) orbital that attachment occurs.

Another experimental result that supports of our proposed model (in particular of what bond is cleaved) has also recently appeared [10]. In these experiments, oligonucleotide tetramers (CGTA and GCTA) were exposed to electrons and the products of irradiation were examined by high-pressure liquid chromatography. The findings of these experiments show primarily cleavage of the phosphodiester (sugar–phosphate C–O) bond in line with our prediction. It should be noted, however, that although this is the first determination by chemical analysis of the products formed in SSBs, the electron energy used (10 eV) was higher than in our simulations. Only at such high energies could enough product be formed to permit the chemical analysis to be carried out. So, although these findings are supportive of our mechanism, it would be nice to have data from such a chemical analysis of products formed by lower-energy electrons.

3. METHODS USED TO CHARACTERIZE THE ENERGIES OF THE METASTABLE ANIONS

3.1. How the rates of bond cleavage are estimated

Before discussing the main tools we use for characterizing metastable electronic states, let us briefly specify how we estimate bond cleavage rates from the energy profiles we generate. For example, from data such as appears in Fig. 4, the rates of C–O bond cleavage

[2] It is possible that, at higher electron energies, attachment to the phosphate P=O π^* or various σ^* orbitals can occur and that SSBs can thereby be formed.

were estimated by taking the C–O vibrational frequency (ca. 10^{13} s^{-1}) and multiplying by the equilibrium Boltzmann probability

$$P = \frac{\exp(-E^*/kT)}{q} \tag{1}$$

that the bond stretches enough to reach the barrier height E^*. As noted earlier, the barrier heights found when electrons are attached to cytosine or thymine range from 0.2 to 1 eV, as a result of which the estimated $T = 298$ K (as in Ref. [6]) C–O bond cleavage rates range from 10^{10} to 10^{-4} s^{-1}. Because the autodetachment rate of a π^* shape resonance is expected to be near 10^{14} s^{-1}, and recalling that we estimated the through-bond electron transfer rates to be ca. 10^{13} s^{-1}, our bond cleavage estimates suggest that at most one in 10^4 nascent π^* anions will undergo C–O bond rupture. Moreover, because we observed that the lower barrier heights E^* occurred when the electron enters the higher-energy component of the π^* resonance, we expect the quantum yield for forming C–O bond fragmentation to be higher at such energies.

Finally, we note that, unlike the case in Refs. [6] and [9] where the DNA was dry, when significant solvation is present, the π^* anion state can be rendered electronically stable (see Fig. 4). In this case, competition between bond cleavage and electron detachment is irrelevant. Instead, transfer of the π^*-attached electron from base to base via the π-stacking framework, which is thought to occur at rates of ca. 10^{12} s^{-1} competes with the bond cleavage rates discussed above. Of course, when strong solvation is present, as it is in living organisms, the phosphate groups will not be rendered neutral by closely associated counter cations as is likely the case in Refs. [6] and [9]. An electron attached to a DNA base adjacent to a negative phosphate unit will not be able to undergo the through-bond electron transfer discussed above because this phosphate group will not provide an attractive potential to the attached electron. Instead, the attached electron likely will migrate through the π-stacking framework to another base. However, even in a solvated environment, a fraction F of the phosphate units have nearby counter cations that render them neutral. Once the attached electron reaches a base near such a neutral phosphate, it has a chance to cause a C–O bond cleavage. The result of solvation then is to reduce the rate of strand breaks from near 10^{10} s^{-1} by the fraction F.

3.2. Stabilization methods

In cases such as we are discussing in this work, the anion formed by near-vertical electron attachment to a base π^* orbital is electronically metastable, but can become electronically stable along the pathway leading to bond cleavage. An example is offered by the data shown in Fig. 4 which pertains to attaching an electron with ca. 1 eV of kinetic energy to a low-energy π^* orbital of cytosine. As the sugar–phosphate C–O bond stretches beyond the barrier at 1.9 Å, the anion potential surface drops below that of the neutral at which point the anion becomes electronically stable. Of course, in this case, at very large C–O distances, the anion lies ca. 5 eV below the neutral because of the extremely high electron affinity of the phosphate group. Although the treatment of the stable anion's Born–Oppenheimer electronic energy can be handled using conventional variational or perturbative methods with standard atomic orbital basis sets, such is not the case at geometries where the anion is electronically metastable. In the latter cases, the anion's resonance state is embedded within a continuum of states corresponding to the neutral molecule plus

a free electron. As such, a rigorous treatment of these resonance states should involve a quantum scattering approach, which, however, is not feasible for the large molecular systems studied here.

For such reasons of practical necessity, hybrid approaches such as the stabilization method [11] and the nuclear charge-scaling method [12] have proven especially useful in determining the energies (i.e., the so-called positions that represent the center of the Heisenberg broadened state) of the resonance states. Let us consider the well known N_2^{-1} shape resonance case to illustrate. Use of the stabilization method (SM) can be thought of as embedding the system of interest within a finite "box" in order to convert the continuum of states corresponding to $N_2 + e^-$ (KE) into discrete states that can be handled using more conventional methods. By then varying the size of the confining box, one can vary the energies of the discrete $N_2 + e^-$ (KE) states. By varying the box size, one of the continuum functions may have its de Broglie wavelength (and thus its KE) changed in a manner that allows this continuum function to match (in value and derivative) the valence-range portion of the N_2^- wave function. It is this combination of valence-range N_2^- and asymptotic-range continuum (properly matched in their values and derivatives) functions that corresponds to the metastable shape-resonance state, and it is the energy where significant valence components develop that provides the stabilization estimate of the state energy.

In the most conventional application of the SM, one uses a conventional atomic orbital basis set that would likely include s and p functions on each N atom, perhaps some polarization d functions and some conventional diffuse s and p orbitals on each N atom. These basis orbitals serve primarily to describe the motions of the electrons within the usual valence regions of space. To this basis, one would append an extra set of diffuse π-symmetry orbitals (because one wishes to study a $^2\Pi_u$ resonance). These orbitals could be p_π (and maybe d_π) functions centered on each nitrogen atom, or they could be d_π orbitals centered at the midpoint of the N–N bond. Either choice can be used because one only needs a basis capable of describing the long-range, $L = 2$ part of the metastable state's wave function. One usually would not add just one such function; rather several functions, each with an orbital exponent α_J that characterizes its radial extent, would be used. Let us assume, for example, that a total of K such π functions have been used.

Next, using the conventional atomic orbital basis as well as the K extra π basis functions, one carries out a calculation in which one computes many energy levels on the N_2^{-1} anion. In this calculation, one tabulates the energies of many (say M) of the electronic states of N_2^{-1}. One then scales the orbital exponents $\{\alpha_J\}$ of the K extra π basis orbitals by a factor $\eta : \alpha_J \rightarrow \eta\alpha_J$ and repeats the calculation of the energies of the M lowest energies of N_2^{-1}. This scaling causes the extra π basis orbitals to contract radially (if $\eta > 1$) or to expand radially (if $\eta < 1$). It is this basis orbital expansion and contraction that produces the expansion and contraction of the "box" discussed above. That is, one does not employ a box directly; instead, one varies the radial extent of the more diffuse basis orbitals to simulate the box variation.

If the conventional orbital basis is adequate, one finds that the extra π orbitals, whose exponents are being scaled, do not affect appreciably the energy of the neutral N_2 molecule. This can be probed by plotting the N_2 energy as a function of the scaling parameter η; if the energy varies little with η, the conventional basis is adequate. In contrast to plots of the neutral N_2 energy vs. η, plots of the energies of the M N_2^{-1} anion states show significant η-dependence as Fig. 8 illustrates.

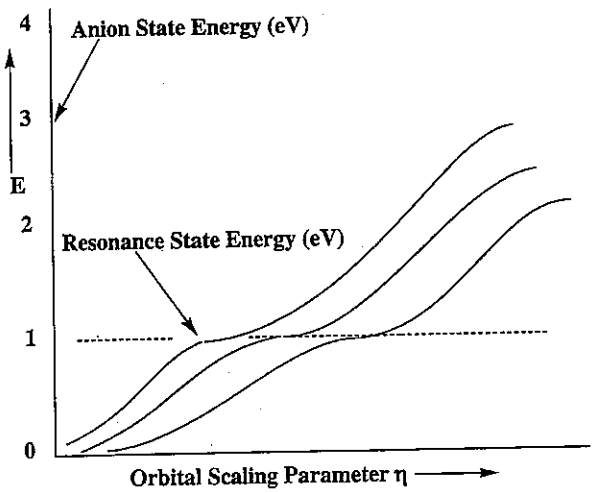

Fig. 8. Plots of the energies of several anion states vs. the orbital scaling parameter η. Note the avoided crossing of state energies near 1 eV.

We should first note that each of the plots of the energy of an anion state (relative to the neutral molecule's energy, which is independent of η) grows with increasing η. This η-dependence arises from the η-scaling of the extra diffuse π basis orbitals. Because most of the amplitude of such basis orbitals lies outside the valence region, the kinetic energy is the dominant contributor to such orbitals' energies. Because η enters into each orbital as $\exp(-\eta\alpha r^2)$, and because the kinetic energy operator involves the second derivative with respect to r, the kinetic energies of orbitals dominated by the η-scaled diffuse π basis functions vary as η^2. It is this quadratic growth with η that is shown in Fig. 8. For small η, all of the π diffuse basis functions have their amplitudes concentrated at large-r and have low kinetic energy. As η grows, these functions become more radially compact and their kinetic energies grow. For example, note the three lowest energies shown above in Fig. 8 increasing from near zero as η grows. As η further increases, one reaches a point at which two of the anion-state energies in Fig. 8 undergo an avoided crossing. At this η value, if one examines the nature of the two wave functions whose energies avoid one another, one finds that one of them contains substantial amounts of both valence and extra diffuse π function character. Just to the left of the avoided crossing, the lower-energy state contains predominantly extra diffuse π orbital character, while the higher-energy state contains largely valence π^* orbital character. In Fig. 8, other avoided crossings occur at higher η-values. For each such crossing, the lower-energy eigenfunction to the left of the avoided crossing contains predominantly extra diffuse π orbital character, while the higher-energy state contains largely valence π^* orbital character.

At any of the special values of η where two states nearly cross, the kinetic energy of the continuum state (as well as its radial size and de Broglie wavelength) are appropriate to connect properly with the valence-region state. It is such boundary condition matching of valence-range and long-range character in the wave function that the stabilization method achieves. So, at such a special η value, one can achieve a description of the shape-resonance state that correctly describes this state both in the valence region and in the large-r region. Only by tuning the energy of the large-r states using the η-scaling can one obtain this proper boundary condition matching.

If one attempts to study such metastable anion states without carrying out such a stabilization study, one is doomed to failure, even if one employs an extremely large and flexible set of diffuse basis functions. In fact, in such a large-basis calculation, one will certainly obtain a large number of anion "states" with energies lying above that of the neutral, but one will not be able to select from these states the one that is the true resonance state. Most of the states will simply be states describing an N_2 molecule with an excess electron at large-r and low KE, but, in the absence of the SM, none will offer a proper description of the metastable state.

In summary, by carrying out a series of anion-state energy calculations for several states and plotting them vs. η, one obtains a stabilization graph. By examining this graph and looking for avoided crossings, one can identify the energies at which metastable resonances occur. It is also possible to use the shapes (i.e., the magnitude of the energy splitting between the two states and the slopes of the two avoiding curves) of the avoided crossings in a stabilization graph to compute the lifetimes of the metastable states. Basically, the larger the avoided crossing energy splitting δE between the two states, the shorter is the lifetime τ of the resonance state and $\tau \approx \hbar/\delta E$.

In our studies of shape resonancesin DNA fragments, we wanted to employ such a stabilization approach. However, as can be deduced from the above discussion, such calculations require the use of quite large atomic orbital basis sets because of the need for many extra diffuse functions whose exponents must be varied. For molecules as large as the DNA fragments we studied, such calculations were simply not feasible. We therefore had to find a different way to characterize the π^* resonance states' electronic wave function. Knowing the energies (i.e., positions) of the low-lying π^* shape resonance states of all four bases from the Burrow-group experiments [7], we decided to employ atomic orbital basis sets on the DNA base to which electron attachment occurs that would generate π^* anion states at the known energies.[3] Specifically, for each of the atoms involved in the base's delocalized π-orbital framework, we scaled the orbital exponents of the most diffuse p_π basis functions by a common amount η and varied η until the energy of the π^*-attached anion (computed at the self-consistent field (SCF) level) relative to that of the neutral matched the desired energy (i.e., as from the data of Ref. [7]). Of course, we also verified that the orbital so obtained has the valence character desired by carrying out a visual inspection. For example, in Fig. 9, we show the cytosine π^* orbital we obtained for the fragment species shown in Fig. 3a; we also show how this orbital evolves as the sugar–phosphate C–O bond is elongated beyond the barrier and the electron transfers through the sugar onto the phosphate unit.

Because we included no extra diffuse basis functions, we were not able to perform true stabilization calculations. Instead, we simply scaled the radial extent of the basis to generate a π^* anion state at the energy we already knew taking care to make sure the resulting state was indeed a base π^* state. Of course, this limited approach precluded being able to estimate the lifetimes of such π^* resonances because our wave function contained only its valence-range component but no continuum component. Although such a "poor man's" stabilization approach should be improved upon in the future, it was the only route available to us at the time.

[3] Actually, because each of the π^* shape resonances have substantial Heisenberg widths, we chose to construct a range of π^* orbitals such that the electron-attached states' energies (relative to the neutral) spanned this range.

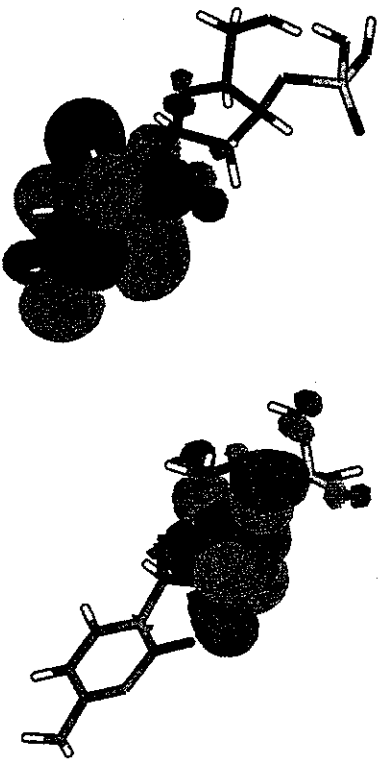

Fig. 9. Plot of the singly-occupied π^* molecular orbital of the fragment shown in Fig. 3a. On the left, this orbital is localized on the cytosine and on the right (at elongated C–O bond length), it has evolved onto the sugar and phosphate. Taken from Ref. [1], Fig. 3.

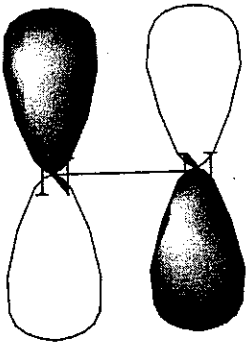

Fig. 10. The π_g^* antibonding orbital of N_2^-.

3.3. Nuclear charge scaling as applied to electron attachment to phosphate P=O π^* orbitals

To explain this technique, let us again consider the $^2\Pi_g$ shape resonance of N_2^-. Due to local valence potentials, there exists an attractive potential that the excess electron experiences while moving in the region of space defined by the π^* antibonding orbital shown in Fig. 10.

However, this potential well is not deep enough to produce a bound state for the excess electron, as a result of which N_2^- is metastable and can spontaneously decay to $N_2(X^1\Sigma_g^+) + e^-$. In contrast, the analogous $^2\Pi$ states of the isoelectronic species NO and

O_2^+ are electronically vertically stable with respect to their corresponding $^1\Sigma^+$ electron-removed species (i.e., vertically, NO lies energetically below NO^+ and O_2^+ below O_2^{2+}). A primary difference underlying this qualitative difference in the ordering of N_2^-/N_2 and the other species is the smaller nuclear charge of N compared to O.

These observations suggest a device that one can use to render metastable shape resonances stable, and thus amenable to conventional (i.e., variational and perturbative) quantum chemistry treatment, while subsequently estimating the energy (position) of the initial metastable state. Specifically, if one increments (by a (small) amount Δq) the nuclear charges of those atoms over which the shape resonance's singly occupied molecular orbital (SOMO) is delocalized,[4] one can differentially stabilize the anion relative to the neutral. If Δq is large enough, the energy of the anion (with nuclear charges increased) will lie below that of the neutral and thus both species' energies can be treated using conventional methods.

So, in the nuclear charge-scaling method, one increases certain nuclear charges by Δq and computes the energies of the neutral and anion. For values of Δq large enough to make the anion lie below the neutral, one plots the energy difference between the anion and the neutral (i.e., the excess electron binding energy). One then extrapolates this plot to $\Delta q \rightarrow 0$ to obtain an estimate of the energy of the metastable anion for the actual molecule (with $\Delta q = 0$). For anions whose energies do not lie much above the neutral (and which tend to be longer lived), one usually finds that very small fractional increments in the nuclear charges are needed. In these cases, the perturbation in the electron-nuclear attraction potential (the electrons are located at $\mathbf{r}_k$ and the nuclei at $\mathbf{R}_a$)

$$V = \sum_a \sum_k \frac{(-\Delta q)}{|\mathbf{r}_k - \mathbf{R}_a|} \tag{2}$$

introduced by replacing certain nuclear charges Z_a by $Z_a + \Delta q$, will be small. Hence, perturbation theory suggests that the shifts in the anion-neutral energy differences should vary linearly with Δq. If larger values of Δq are needed to make the anion stable, the plots in the anion-neutral energy differences can display significant quadratic (in Δq) character; in these cases, extrapolation is carried out using a second order (in Δq) polynomial but only for values of Δq where the anion is stable.

An example of the use of this nuclear charge scaling device is provided in our study of electron attachment to the P=O π^* orbital of the sugar–phosphate–sugar unit some data of which is shown in Fig. 3c. As shown in Fig. 3c, subsequent to electron attachment, either of two sugar–phosphate C–O bonds (labeled 3′ and 5′) can rupture. In Fig. 11 we show plots of the energies of the neutral and electron-attached species as functions of the C–O bond lengths for the cases in which the 3′ C–O bond is ruptured or the 5′ C–O bond breaks. For the anion, two energy curves are shown. One relates to the excess electron residing in the P=O π^* orbital and the second pertains to the excess electron being in the σ^* orbital of the C–O bond being cleaved. To obtain the data shown at C–O bond lengths where the anion

[4] It is not always necessary to place the stabilizing excess charge on the nuclei where the excess electron is localized. For example, in our study of the metastable SO_4^{2-} dianion, we increased the charge on sulfur. We made this choice because all four oxygen atoms in this species are equivalent and we did not wish to induce artificial symmetry breaking (see first references in Ref. [13]). On the other hand, when we recently studied the ground and (metastable) excited states of the O_2^- anion, we increased both oxygen atoms' charges (see second reference in Ref. [13]).

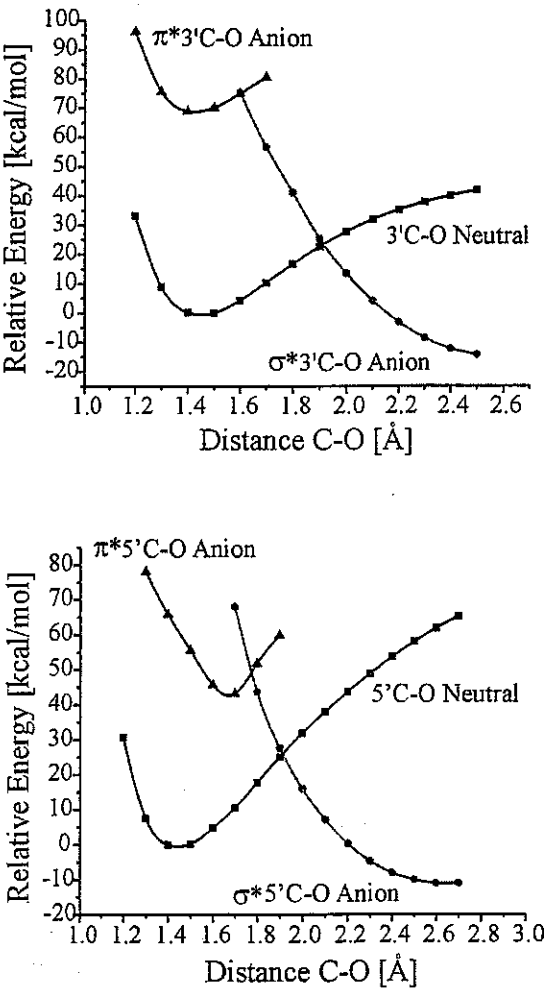

Fig. 11. Energies of the neutral, π^*-attached anion, and σ^*-attached anion as functions of the 3′ C–O (top) and 5′ C–O (bottom) C–O bond lengths. Taken from Ref. [4], Fig. 3.

curves lie above the neutral, we used the nuclear charge scaling device detailed above as we now discuss.

To illustrate the data used to extrapolate (to $\Delta q \rightarrow 0$) the anion-neutral energy plots for all values of the C–O bond lengths where the anion is metastable, we shown in Fig. 12 four such plots applying to the 3′ and 5′ cases and to the σ^* and π^* anions.

To further illustrate the utility of the nuclear charge-scaling device, we show in Fig. 13 the P=O π^* and C–O σ^* orbitals obtained when the phosphorous and oxygen nuclear charges are increased by 0.5 for the four cases whose Δq plots are shown in Fig. 12.

Before ending this section, let us return to Fig. 11 to discuss what we learned from the study relating to attaching an electron to a P=O π^* orbital. First, our data suggest that electrons in the range of 2 eV will be required to attach to such an orbital. In Ref. [9], DNA strand breaks were observed with electrons below 1 eV, so these breaks likely did not involve attachment to P=O π^* orbitals. Moreover, even when electrons of 2 eV energy or more attach to P=O π^* orbitals, evolution of this anion along the either the 3′ or 5′ C–O bond elongation to produce bond cleavage requires surmounting a barrier of ca. 1 eV (see Fig. 11 where the π^* and σ^* anion curves cross). Our earlier work showed that the barriers associated with C–O bond cleavage subsequent to base π^* orbital-attachment were much

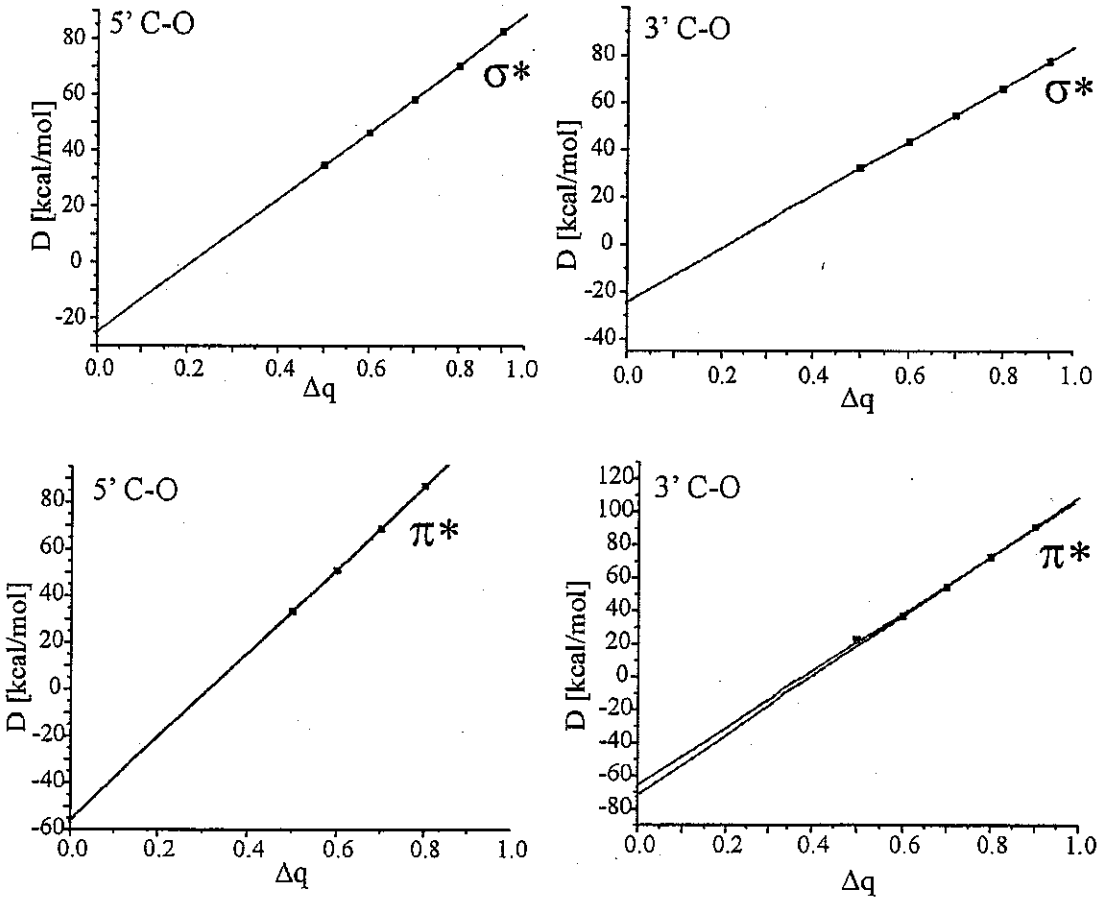

Fig. 12. SCF-level electron binding energy plots for the π^* (bottom) and σ^* (top) anions for certain values of the 3′ or 5′ C–O bond lengths at all of which the anion is metastable. Specifically, for the π^* anion $R = 1.4$ Å for the 3′ and 1.5 Å for the 5′; for the σ^* anion $R = 1.8$ Å for both the 3′ and 5′ cases. In the 3′ C–O π^* plot, displays considerable curvature, we show two linear fits to give some idea of the uncertainty. Taken from Ref. [2], Fig. 6.

lower. Therefore, we believe it unlikely that much of the strand break damage to DNA occurs by P=O π^* bond attachment when the electron has a kinetic energy in the 0.1–2 eV range.

4. SUMMARY

In this paper, we used several of our recent studies to illustrate the mechanisms by which very low-energy (0.1–2 eV) free electrons attach to DNA to cause strong (ca. 4 eV) covalent bonds to break. We also used these examples to illustrate the special tools we use for probing metastable electronic states. The primary conclusions of this body of work have been that (i) attachment to base π^* orbitals to form shape resonances in the 0.1–2 eV energy range most likely results in cleavage of sugar–phosphate C–O σ bonds, (ii) the thermodynamic driving force for this process is the large electron affinity of the phosphate unit, (iii) the rates of C–O bond cleavage can be as high as 10^{10} s^{-1} and are determined by the rate at which an energy barrier on the anion's potential surface is surmounted, (iv) bond cleavage initiated by electron attachment to phosphate P=O π bonds is less likely involved.

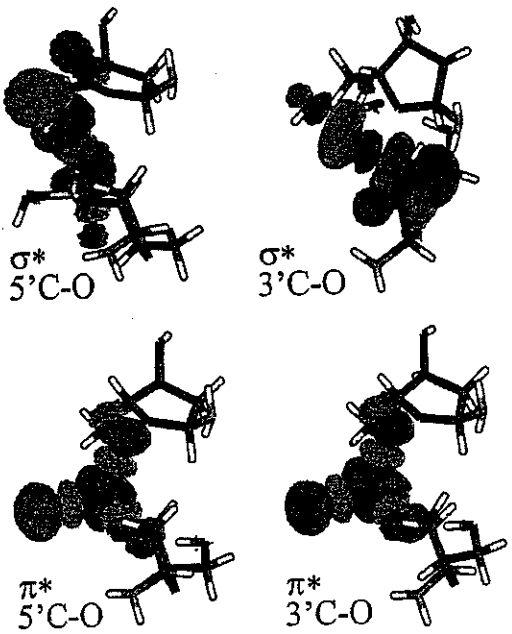

Fig. 13. The π^* and σ^* orbitals corresponding to the four cases detailed in Fig. 12 as the P and O charges are increased by 0.5. Taken from Ref. [2], Fig. 8.

and (v) the through-bond electron transfer from the base to the C–O σ bond occurs at ca. 10^{13} s^{-1} and thus is not rate-limiting. Finally, subsequent to our works in which these predictions were offered, very recent experiments have appeared in which (i) convincing evidence is given in support of our claim that 0.1–2 eV electrons attach to base π^* orbitals rather than to P=O π^* or any σ^* orbitals, and (ii) chemical analysis of the products of strand breaks shows that it is indeed primarily the sugar–phosphate C–O bond that breaks.

Before closing, it is worth noting that an excellent review appeared recently [14] covering much of the recent history of studies related to electron-induced strand breaks in DNA. In that review, work on electron-induced bond cleavage in DNA bases (where H atom elimination and base radical anion formation occurs), in base-sugar units (where cleavage of the bond connecting the base to the sugar occurs), and in sugar–phosphate units (where the sugar–phosphate C–O bond cleaves) is overviewed. In addition, the potential role of dipole-bound states in effecting the initial electron attachment is also discussed in Ref. [14].

ACKNOWLEDGEMENTS

Support of the National Science Foundation through grant CHE 0240387 is appreciated as is significant computer time provided by the Center for High Performance Computing at the University of Utah.

REFERENCES

[1] R. Barrios, P. Skurski, J. Simons, *J. Phys. Chem. B* **106** (2002) 7991–7994.
[2] J. Berdys, I. Anusiewicz, P. Skurski, J. Simons, *J. Am. Chem. Soc.* **126** (2004) 6441–6447.
[3] J. Berdys, I. Anusiewicz, P. Skurski, J. Simons, *J. Phys. Chem. A* **108** (2004) 2999–3005.

[4] I. Anusiewicz, J. Berdys, M. Sobczyk, P. Skurski, J. Simons, *J. Phys. Chem. A* **108** (2004) 11381–11387.
[5] J. Berdys, P. Skurski, J. Simons, *J. Phys. Chem. B* **108** (2004) 5800–5805.
[6] B. Boudaiffa, P. Cloutier, D. Hunting, M.A. Huels, L. Sanche, *Science* **287** (5458) (2000) 1658–1662.
[7] K. Aflatooni, G.A. Gallup, P.D. Burrow, *J. Phys. Chem. A* **102** (1998) 6205–6207.
[8] X. Li, M.D. Sevilla, L. Sanche, *J. Am. Chem. Soc.* **125** (2003) 13668–13669.
[9] F. Martin, P.D. Burrow, Z. Cai, P. Cloutier, D. Hunting, L. Sanche, *Phys. Rev. Lett.* **93** (2004) 068101.
[10] Y. Zheng, P. Cloutier, D. Hunting, L. Sanche, J.R. Wagner, *J. Am. Chem. Soc.* **127** (2005) 16592–16598.
[11] A.U. Hazi, H.S. Taylor, *Phys. Rev. A* **1** (1970) 1109–1116;
J. Simons, *J. Chem. Phys.* **75** (1981) 2465–2467;
J. Simons, Roles Played by Metastable States in Chemistry, in: *Resonances in Electron–Molecule Scattering, Van der Waals Complexes, and Reactive Chemical Dynamics*, in: *ACS Symposium Series*, vol. 263, 1984, pp. 3–16;
R.F. Frey, J. Simons, *J. Chem. Phys.* **84** (1986) 4462–4469.
[12] B. Nestmann, S.D. Peyerimhoff, *J. Phys. B* **18** (1985) 615–626;
B. Nestmann, S.D. Peyerimhoff, *J. Phys. B* **18** (1985) 4309–4319.
[13] A. Whitehead, R. Barrios, J. Simons , *J. Chem. Phys.* **116** (2002) 2848–2851;
K.M. Ervin, I. Anusiewicz, P. Skurski, J. Simons, W.C. Lineberger, *J. Phys. Chem. A* **107** (2003) 8521–8529.
[14] L. Sanche, *Eur. Phys. J. D* **35** (2005) 367–390.